Build Simul (2024) 17: 1557–1578
https://doi.org/10.1007/s12273-024-1142-5

Exercise and resting periods: Thermal comfort dynamics in gym environments

Ali Berkay Avci[1] (✉), Görkem Aybars Balci[2], Tahsin Basaran[1]

1. Department of Architecture, Faculty of Architecture, Izmir Institute of Technology, Urla, Izmir, Türkiye
2. Department of Coaching Education, Faculty of Sport Sciences, Ege University, Bornova, Izmir, Türkiye

Abstract

Physical exercise spaces emerged as popular facilities due to recognizing the significance of physical well-being. This study investigates the relationship among physiological responses, human body energy transfer modes, and indoor environmental conditions in influencing thermal comfort perception within indoor physical exercise space. Seven male participants engaged in a 30 min constant-work-rate cycling exercise and a 20 min resting period in a climatic chamber. The physiological and environmental responses were recorded during the experiments, and the body's energy transfer modes were calculated using the collected data. The dataset was prepared using the 2 min averages of the collected data and calculated parameters across the experiment phases, including the features of skin temperature, core temperature, skin relative humidity, heart rate, oxygen consumption, body's heat transfer rates through convection, radiation, evaporation, and respiration, net metabolic heat production rate (metabolic rate minus external work rate), indoor air temperature, indoor relative humidity, air velocity, and radiant temperature. Gradient boosting regressor (GBR) was selected as the analyzing method to estimate predicted mean vote (PMV) and thermal sensation vote (TSV) indices during exercise and resting periods using features determined in the study. Thus, the four GBR models were defined as PMV-Exercise, PMV-Resting, TSV-Exercise, and TSV-Resting. In order to optimize the models' performances, the hyperparameter tuning process was executed using the GridSearchCV method. A permutation feature importance analysis was performed, emphasizing the significance of net metabolic heat production rate (24.2%), radiant temperature (17.0%), and evaporative heat transfer rate (13.1%). According to the results, PMV-Exercise, PMV-Resting, and TSV-Resting GBR models performed better, while TSV-Exercise faced challenges in predicting exercise thermal sensations. Critically, this study addresses the need to understanding the interrelationship among physiological responses, environmental conditions, and human body energy transfer modes during both exercise and resting periods to optimize thermal comfort within indoor exercise spaces. The results of this study contribute to the operation of indoor gym environments to refine their indoor environmental parameters to optimize users' thermal comfort and well-being. The study is limited to a small sample size consisting solely of male participants, which may restrict the generalizability of the findings. Future research could explore personalized thermal comfort control systems and synergies between comfort optimization and energy efficiency in indoor exercise spaces.

Keywords

physical exercise
gradient boosting
thermoregulation
fitness
thermal comfort

Article History

Received: 19 March 2024
Revised: 22 April 2024
Accepted: 07 May 2024

1 Introduction

Increasing recognition of the significance of physical well-being in contemporary life conveyed the rise in popularity of indoor exercise spaces, such as gyms and fitness centers. According to the European Health and Fitness Market 2022 report, the number of fitness club members grew by 2% in Europe compared to the previous year, culminating in

E-mail: aliavci@iyte.edu.tr; aliavci@sdu.edu.tr

List of symbols

A_D	Dubois body area (m^2)
C	convective heat loss from skin (W/m^2)
$\mathbf{e}_b$	error of the base model
$\mathbf{e}_p$	new error estimate
E_{sk}	evaporative heat loss from skin (W/m^2)
$F(\mathbf{x})$	final prediction
$f_j(\mathbf{x})$	prediction of the j^{th} weak model
h_a	enthalpy of ambient air (J/kg)
h_c	convective heat transfer coefficient ($W/(m^2 \cdot K)$)
h_{cc}	corrected convective heat transfer coefficient ($W/(m^2 \cdot K)$)
h_e	evaporative heat transfer coefficient $W/(m^2 \cdot K)$
h_{ex}	enthalpy of exhaled air (J/kg)
h_r	radiant heat transfer coefficient ($W/(m^2 \cdot K)$)
HR	heart rate (bpm)
I_{cl}	clothing insulation (clo)
$\mathbf{I}_x$	feature importance value
L	loss or error function
LR	Lewis ratio, the equivalent of 16.5 K/kPa
M	rate of metabolic heat production (W/m^2)
J	number of weak models
m	body mass (kg)
MAE	mean absolute error
met	metabolic rate level during resting, the equivalent of 58 W/m^2
$\dot{m}_{res}$	pulmonary ventilation rate (kg/s)
MSE	mean squared error
p_a	water vapor pressure at ambient air (kPa)
PMV	predicted mean vote
$p_{sk,s}$	water vapor pressure at skin, assumed to be at saturated vapor pressure (kPa)
p_t	local atmospheric pressure (kPa)
Q_{res}	total rate of heat loss through respiration (W/m^2)
QO_2	oxygen consumption rate (mL/s)
R	radiative heat loss from skin (W/m^2)
RH	relative humidity (%)
RH_{in}	indoor relative humidity (%)
RH_{sk}	skin relative humidity (%)
RER	respiratory exchange rate
S	rate of total heat storage in skin and core compartments (W/m^2)
T_a	air temperature (°C)
t	time (s)
T_{cr}	core temperature (°C)
T_{in}	indoor air temperature (°C)
T_{sk}	skin temperature (°C)
TSV	thermal sensation vote
T_{rad}	radiant temperature (°C)
V	mean indoor air velocity (m/s)
$VO_{2,max}$	maximal oxygen uptake (mL/(min·kg))
VCO_2	carbon dioxide production (mL/(min·kg))
VO_2	oxygen intake, in O_2 mL/(kg·min)
w	skin wettedness
W	rate of mechanical work accomplished (W/m^2)
$\mathbf{X}$	dataset
$\mathbf{x}$	feature
$\mathbf{X}_{perm}$	new feature matrix
y_i	actual value
$\tilde{y}_i$	predicted value
γ_j	scaling factor assigned to the j^{th} model
σ	Stefan-Boltzmann constant, the equivalent of 5.67×10^{-8} $W/(m^2 \cdot K^4)$
ε	emissivity of the skin, the equivalent of 0.95

Abbreviations

CO_2	carbon dioxide
GBR	gradient boosting regressor
O_2	oxygen

56.3 million individuals (Deloitte 2022). This escalating indoor exercise trend can be attributed to the appeal of controlled indoor environments, offering a reliable alternative to the unpredictable fluctuations of outdoor climates (Sevilmis et al. 2023). However, it is essential to recognize that while indoor exercise facilities provide a predictable climate conducive to physical activity, they also present challenges related to energy consumption, indoor air quality, and thermal comfort (Cui et al. 2024).

During physical exercise, the human body releases higher amounts of metabolic heat, moisture, and CO_2 into the surrounding environment compared to sedentary activities (Zhai et al. 2020). Ensuring a healthy, productive, and comfortable exercise environment necessitates adequate fresh air supply rates and maintenance of thermal comfort conditions (Avci et al. 2024). Consequently, indoor exercise spaces heavily rely on heating, ventilation, and air conditioning (HVAC) systems to regulate thermal conditions, despite the significant energy consumption and environmental impacts associated with their operation (Kapalo et al. 2021). Therefore, it is imperative to elucidate the effects of factors influencing thermal comfort during exercise to enable the provision of optimal indoor environmental conditions in indoor gym environments.

Thermal comfort, the state of mind that expresses satisfaction with the surrounding thermal environment,

depends on the energy balance between the occupants' body and environment (ASHRAE 2020). During physical exercise, the rate of metabolic energy production increases. While a limited portion of this energy rate is utilized for mechanical work by the muscles during exercise, the remainder is released to the environment through body energy transfer modes, including respiration (latent and sensible), sweat evaporation, radiation, and convection (Parsons 2014). These energy transfer processes of the body are directly influenced by four critical indoor environmental factors: indoor air temperature, relative humidity, radiant temperature, and air velocity. Determined by utilizing the relationships between these factors, the predicted mean vote (PMV) index is commonly employed as a widely accepted indicator for the objective evaluation of thermal comfort in steady-state indoor conditions (Fanger 1970; Amaripadath et al. 2023). As the body experiences dynamic thermal conditions during exercise, studies frequently incorporate the thermal sensation vote (TSV) as a supplementary subjective assessment tool, enhancing the evaluation of thermal comfort alongside the PMV index (Zhang et al. 2019; Huang et al. 2022; Shi et al. 2022).

Understanding the effects and relationships among the body's thermal responses, indoor environmental conditions, and heat exchange modes is crucial for establishing and maintaining thermal comfort. Investigating the thermal dynamics in indoor exercise spaces is crucial for several reasons. Firstly, it directly impacts the well-being and comfort of individuals engaging in physical activities, which is paramount for encouraging regular exercise and maintaining overall health (Gao et al. 2023). Additionally, optimizing indoor thermal conditions can enhance the effectiveness of workout sessions by ensuring optimal comfort levels, thereby potentially improving exercise performance and adherence to fitness routines (Huang et al. 2021). Moreover, gaining insights into the interplay between physiological responses, environmental factors, and thermal comfort perception can inform the design and operation of indoor exercise facilities (Cui et al. 2024). By identifying key factors influencing thermal comfort, this research has the potential to guide the development of more energy-efficient HVAC systems tailored to indoor exercise environments (Avci et al. 2024). Furthermore, understanding how different exercise and resting periods affect thermal comfort can lead to the implementation of targeted strategies to enhance comfort during both phases, ultimately promoting a more enjoyable and sustainable exercise experience (Zhou et al. 2023). Several studies focused on thermal comfort conditions during exercise and highlighted the limitations of the PMV index for dynamic thermal conditions with higher metabolic heat production rates (Zhai et al. 2015; Vargas et al. 2018; Wang et al. 2022). Jia et al. (2023) examined subjective perceptions and physiological parameters during transitions between sitting and walking, finding increased sensitivity to core temperature changes in downward activity shifts. Their study also noted prolonged heat dissipation and heightened subjective thermal evaluation (TSV) following 20 min moderate-intensity activities (2.2–3.4 met). Another study by Lin et al. (2023) investigated the effects of exercise intensity and thermal environment on thermal responses, revealing significant impacts on heart rate and metabolic rate during exercise. They found that PMV underestimated the metabolic rate of moderate-to-high intensity exercise by at least 9.7%, which emphasized the need for a comprehensive understanding of evaluating thermal responses during exercise. Similarly, Zhang et al. (2020c) revealed that the human body takes 3–5 minutes to reach a new metabolic level after walking and 4–5 minutes to return to a normal sedentary state from exercise, and their findings underscored the influence of airflow disturbances caused by walking on thermal comfort. Additionally, Zhou et al. (2021) developed a thermal sensation model that demonstrated promising accuracy in predicting thermal perception under various outdoor scenarios, particularly with sudden changes in solar radiation, offering insights into thermal assessment in specific contexts. Moreover, their new model showed trends in thermal changes, even though it had slightly less accuracy than the PMV model in environments with indoor temperature gradients/sudden changes.

These previous studies have focused on determining thermal comfort and affecting physical and physiological factors during different exercise intensities. However, few studies have yet to pay enough attention to the proceeding resting state of the body after the exercise phase. This understanding gains additional significance when considering the impact of both exercise and resting periods on thermal comfort within exercise spaces. The necessity to analyze exercise and resting periods separately arises from the recognition that exercise spaces accommodate not only physical activity but also periods of rest. It is also because the body requires at least as long time as the exercise period in the resting period to release the heat stress stored inside the body after the exercise, as highlighted by the previous studies (Kenny et al. 2008; Kenny and McGinn 2017; Périard et al. 2021). Therefore, as much as the exercise, the resting period also requires special attention in terms of thermal comfort. Moreover, the application of machine learning techniques emerges as pivotal in predicting thermal comfort and identifying the influencing key factors (Qavidel et al. 2022; Yang et al. 2022a). Machine learning's potential to identify non-linear complicated relations at broader perspectives has made it frequently preferred by thermal comfort studies (Wang et al. 2019; Zhou et al. 2020; Li et al.

2023). While existing studies have focused on predicting thermal comfort during exercise, few have delved into the distinct impacts of exercise and resting periods on thermal responses. Similarly, the application of machine learning techniques remains relatively unexplored in the context of thermal comfort during physical exercise indoors. Therefore, this study aims to address this notable gap by examining the distinct impacts of both exercise and resting periods on thermal comfort.

The study seeks to assess the feasibility and accuracy of predicting PMV and TSV values within physical activity spaces through the application of the gradient boosting regressor (GBR) model. This assessment is conducted via a comprehensive case study involving seven male participants, encompassing both exercise and resting periods. The investigation spans subjective and objective thermal comfort indicators, exploring their correlations with energy transfer modes, environmental variables, and physiological responses. Through this examination, the study aims to unveil key features within indoor exercise environments. The findings derived from this case study of seven individuals are poised to contribute to the field of thermal comfort research by providing a foundational framework for forthcoming inquiries encompassing more extensive and diverse participant samples.

The following sections will detail the methodology employed in the experimental study and data collection (Section 2), including the laboratory setting's relevance to gym environments, test procedures, measurements of physiological and environmental data, calculations of human body energy rate modes, thermal comfort indices, and the refined dataset. Section 3 will present the construction and assessment of the machine learning model, including model performance assessment, hyperparameter tuning, and interpretation of feature importance analysis. Results will be discussed in Section 4, covering descriptive data analysis, thermal comfort indices during exercise and resting periods, performance of the GBR models, and feature importance analysis. Section 5 will address limitations and propose future directions for research. Finally, Section 6 will provide concluding remarks summarizing the study's findings and implications.

2 Methods

2.1 Experimental study and data collection

The experiments of this study were conducted in a climate-controlled room (Figure 1(a)) with normothermic and normoxic conditions. The temperature, relative humidity, and CO_2 levels were monitored and regulated as 21±0.3 °C, 43%±4%, and below 450 ppm, respectively. The test chamber's floor area is four by six meters, and its height is three meters. The case study was conducted by seven males (ages 18–28) who had undertaken a 30 min cycling exercise and a 20 min resting phase. The participants had an average height of 1.77 m, mass of 72 kg, $VO_{2,max}$ of 51±7 mL/(min·kg) (explained in Section of 2.1.1). They were included in the experiments with short pants, socks, and sports shoes to leave a larger skin area for thermal camera measurements (Figure 1(b)). The study's experimental protocols underwent approval from the Ethics Committee for Medical Research at the Medical School of Ege University, identified by report number 22-9.1T/20.

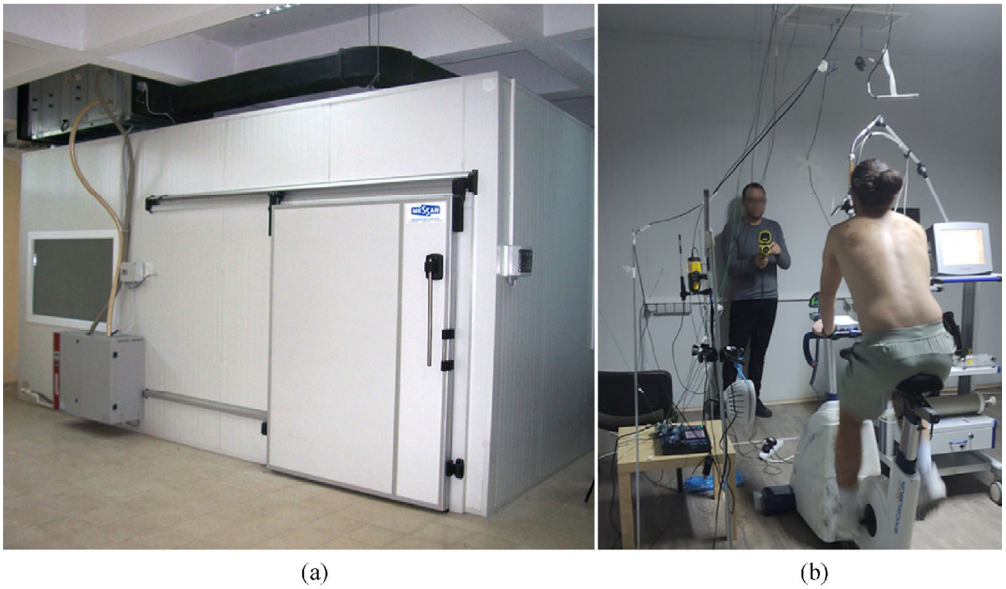

(a) (b)

Fig. 1 Experiment room (a) outside view and (b) inside view with experimental measurements

2.1.1 Laboratory setting and its relevance to gym environments

The experiments detailed in this study were conducted within a controlled laboratory environment, chosen for its capacity to replicate key aspects of gym environments while allowing for precise control over experimental conditions. While the setting differed from real-world gym facilities, it was selected to ensure consistency and reproducibility across trials. The laboratory setting facilitated the manipulation of environmental variables such as temperature, relative humidity, air velocity, fresh air supply, enabling the simulation of conditions commonly encountered in indoor exercise spaces. This approach was instrumental in providing a standardized platform for investigating thermal comfort dynamics during physical activity. Additionally, the laboratory environment afforded a safe and controlled setting for participants, minimizing external variables that could potentially impact the study outcomes. While the laboratory setting may not fully capture every nuance of real-world gym environments, efforts were made to replicate the most salient features relevant to thermal comfort.

2.1.2 Test procedures

The experimental design of this study in a controlled room follows a comparative approach, building upon methodologies from previous research (Balci et al. 2016; Zora et al. 2017; Avci et al. 2024; Balci et al. 2024). Each participant was in the experiment room for 4 sessions, as follows:

Familiarization sessions

Familiarization sessions were conducted in the experiment room to introduce participants to the measurement devices and the protocols. Firstly, the anthropometric measurements of the participants were taken. Following this step, a 5 min, 4-stage exercise test was performed at a cadence of 80–90 rpm, starting with an estimated workload of 80 W and increasing in 30 W increments. The main aim of this session was to determine the initial work rate of the submaximal VO_2 tests. Heart rate (HR) was recorded during the test.

Submaximal VO_2 tests

Submaximal tests commenced 24–48 hours following the familiarization sessions, employing a work rate set around 50% of their maximal HR that was calculated from earlier sessions. The 4-stage test adopted 5 min intervals and incorporated load augmentations of 30 W in each stage. The test was concluded with load adjustments that ensured they remained below 80% of their maximal HR reserve, as determined by the Karvonen reserve HR formula. The purpose of the submaximal VO_2 tests was to calculate the work-load corresponding to approximately 70% of the maximal heart rate reserve to determine the initial load of the maximal VO_2 test.

Maximal VO_2 tests

Following a 60 min break time, maximal VO_2 tests were carried out to determine the load of the submaximal constant work rate exercise test by calculating the maximal oxygen consumption level. The test started with the work rate equivalent to 70% of the maximal HR reserve and continued with the work rate increments of 30–20 W every 2 minutes until the task failure. The means of the last 30 seconds of the steps were recorded for all parameters. The highest 30 seconds means of VO_2 and corresponding work rate were noted.

Submaximal constant work rate exercise

After a 24 to 48 hour interval following the maximal VO_2 tests, participants were summoned for the submaximal constant work rate exercise trials, which constitute the main experimental test sessions where the required data were gathered for the study. After a 10 min waiting period to ensure thermal equilibrium within the experiment room, participants undertook a 30 min session of submaximal exercise at a consistent work rate equivalent to 60% of their maximal VO_2. After the submaximal constant work rate exercise sessions had been finished, the participants rested for 20 minutes. The participants were asked to stay on the stationary bike while resting. The related data of the exercise period used in this study were collected in this submaximal constant work rate exercise session. Throughout the duration of the 30 min constant work rate exercise tests and 20 min resting period, parameters including oxygen intake (VO_2), carbon dioxide production (VCO_2), HR and respiratory exchange ratio (RER), skin temperature (T_{sk}), core temperature (T_{cr}), and skin relative humidity (RH_{sk}) variables were measured continuously and averaged at 2 min intervals.

2.1.3 Measurement of physiological and environmental data

Physiological and environmental data measurements were done during submaximal constant work rate exercise and resting periods of the experiments, following the methodologies of previous research (Balci et al. 2016; Zora et al. 2017; Avci et al. 2024; Balci et al. 2024). The collected physiological data involves T_{sk}, RH_{sk}, T_{cr}, HR, VO_2, VCO_2, RER, and external work rate (W). The environmental data collected inside the experiment room are indoor air temperature (T_{in}), mean radiant temperature (T_{rad}), mean indoor air velocity (V), and indoor relative humidity (RH_{in}). The locations of the measurement devices are given in Figure 2, and their details are provided in Table 1. The measurement devices of the main parameters are listed as follows.

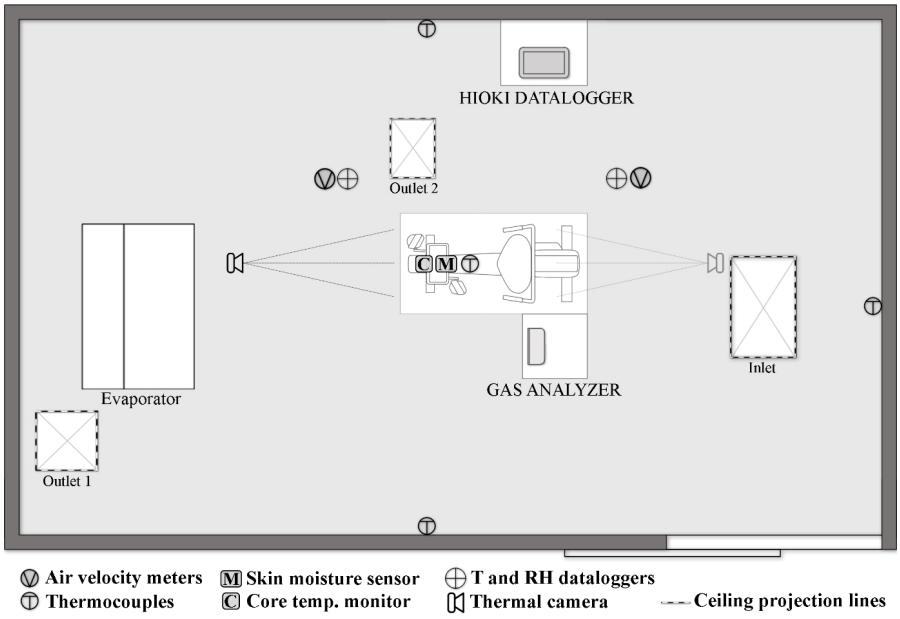

Fig. 2 Locations of the measurement devices—schematic plan of the experiment room

Table 1 Details of the measurement tools and sensor

Device	Brand/model	Origin country/state	Sensitivity/accuracy
Body mass and height monitor	Seca 767	USA	Height: ±0.5 cm or ±0.1 cm Weight: ±0.1 kg
Telemetric heart rate monitor	Polar RS 400, Polar Electro Oy	Kempele, Finland	± 1% or 1 bpm
Gas analyzer	Innocor INN00500, Innovision A/S	Odense, Denmark	—
Work rate expenditure monitoring, Sport Cycling ergometer with electro-magnetic mechanism braking	Lode BV, Excalibur Sport, Lode Medical Technology	Groningen, the Netherlands	—
Lactate Analyzer	Biosen C-line, EKF Diagnostics GmbH	Barleben, Germany	VK ≤ 1.5 % (12 mmol/L)
Digital Barometer	TFA Dostmann	Germany	+3 hPa (950 hPa @ +20 °C–30 °C)
Infrared thermal camera	Trotec IC080L	Germany	±0.05 °C
Digital moisture monitor	DMM	China	±1%
Swallowable core temperature sensors	Bodycap e-Celsius	Normandy, France	±0.2 °C
Air velocity meter	Trotec TA300	Germany	±5% m/s
K- and T-type thermocouples	Verth	—	±0.1 °C
Data reader, transmitter, and storage device	Memory Hilogger, HIOKI LR 8402-20	—	—
Temperature and relative humidity datalogger	AZ7798	China	±0.6 °C, ±3%

- T_{cr} responses were recorded by swallowable temperature sensors that transmit telemetry data to a monitor recording the responses at 10 s intervals (e-Celsius Performance Pill; ±0.2 °C).
- T_{sk} responses were recorded by an infrared thermal camera (384 pixel × 288 pixel, ±0.05 °C < 80 °C, Trotec IC080L) at 2 min intervals. The skin temperature data used in the study were averages of the chest and back regions of the participants.
- RH_{sk} measurements were conducted using a digital moisture monitor (DMM, ±1%) employing bioelectric impedance analysis (BIA) to accurately assess skin moisture levels. The device recorded RH_{sk} on the chest and back of the body at 2 min intervals. The recorded RH_{sk} data used in the study as the averages of these two regions.
- A gas analyzer (Innocor INN00500, Innovision A/S) was used to record variables regarding respiratory gases at 5 s intervals.
- External work rates of the participants were controlled by a sport bike ergometer with an electromagnetic braking

mechanism (Lode BV, Excalibur Sport, Lode Medical Technology).

- T_{in} and RH_{in} were measured by 2 pieces of temperature and humidity datalogger (AZ7798, ±0.6 °C, ±3%) at 5 s intervals.
- Two air velocity meters (Trotec TA300, ±5% m/s) was used to record indoor air velocity (V) data inside the experiment room at 5 s intervals.
- T_{rad} responses were collected as the average temperatures of each surface's center-point in the experiment room (walls, ceiling, and floor), which were measured by copper-constantan and nickel-based thermocouples (±0.1 °C) connected to a HIOKI LR 8402–20 datalogger.

2.1.4 Calculations of human body energy rate modes

In this study, necessary heat transfer modes are calculated using ASHRAE's human body energy balance equations (ASHRAE 2009), as given in Equation (1). According to the equation, the energy production rate inside the body (M) turns into mechanical work rate (W) for the muscles. The rest of the energy is released to the environment through convection (C), radiation (R), sweat evaporation (E_{sk}), and respiration (Q_{res}). The residual portion that cannot be simultaneously transferred to the environment is stored inside the body (S).

$$M - W = C + R + E_{sk} + Q_{res} + S \tag{1}$$

The indirect calorimetry approach is implemented to provide the metabolic rate values in the study, as shown in Equation (2) (Nishi 1981). The body surface area (A_D) were derived from the Dubois formula based on the participants' height and mass (Du Bois and Du Bois 1989). In Equation (2), RER represents the respiratory gas exchange rate calculated by the ratio of CO_2 production to O_2 consumption. The overall oxygen consumption rate of an individual in mL/s is denoted by QO_2.

$$M = 21 \times (0.23 \times \mathrm{RER} + 0.77) \frac{\mathrm{QO_2}}{A_D} \tag{2}$$

The energy transfer rates by respiration were calculated using the air mass ($\dot{m}_{res}$) exhaled per second and the difference between the enthalpy of the air exhaled (h_{ex}) and inhaled (h_a), as shown in Equation (3) (ASHRAE 2009). The values of h_{ex} and h_a were determined using a psychrometric chart, based on the relative humidity and temperature of the exhaled air and the ambient air inside the room at 2 min intervals.

$$Q_{res} = \frac{\dot{m}_{res}(h_{ex} - h_a)}{A_D} \tag{3}$$

Evaporative energy release rates from the skin were calculated using the difference between water vapor pressure at the body surface ($p_{sk,s}$) and the partial water vapor pressure of the indoor air (p_a) , the ratio of skin wettedness (w), and the coefficient of evaporative energy transfer (h_e). The values of $p_{sk,s}$ and p_a were determined using a psychrometric chart, based on the relative humidity and temperature of the skin (RH_{sk} and T_{sk}) and the ambient air inside the room (T_{in} and RH_{in}) at 2 min intervals. The convective heat transfer coefficient (h_c) values were determined using Equation (6), based on the indoor air velocity (V) levels measured at 2 min intervals. Then, the h_e values were calculated using the h_c values with the Lewis ratio (LR) as presented in Equation (5). Considering that the participants wore only short pants and shoes, E_{sk} values in this study were obtained, as presented in Equation (4) (ASHRAE 2009).

$$E_{sk} = w \times h_e \times (p_{sk,s} - p_a) \tag{4}$$

$$\mathrm{LR} = \frac{h_e}{h_c} \tag{5}$$

$$h_c = 8.3 \times V^{0.6} \tag{6}$$

Convective and radiative energy transfer modes were derived as presented in Equations (7) and (8) (ASHRAE 2009). The convective energy release rate from the skin is based on the difference between T_{sk} and T_a and the corrected convective heat transfer coefficient (h_{cc}). The h_{cc} values were approximated using the h_c values and local atmospheric pressure (p_t) at 2 min intervals, as presented in Equation (9). On the other hand, the dissipation rate of radiant energy relies on the variation in T_{sk} and T_{rad}, along with the radiant heat transfer coefficient (h_r). The h_r values were calculated using emissivity of the skin (ε), Stefan- Boltzmann constant (σ), T_{sk}, and T_{rad} parameters, as presented in Equation (10). Once the combined energy transfer values from respiration and skin were obtained, the total rates of required energy storage within the body (S) given in Equation (2) were determined by deducting this value from the net rate of metabolic energy production.

$$C = h_{cc}(T_{sk} - T_a) \tag{7}$$

$$R = h_r(T_{sk} - T_{rad}) \tag{8}$$

$$h_{cc} = h_c \left(\frac{p_t}{101.33}\right)^{0.55} \tag{9}$$

$$h_r = 4\varepsilon\sigma\left(273.2 + \frac{T_{sk} + T_{rad}}{2}\right)^3 \tag{10}$$

2.1.5 Thermal comfort indices

In order to evaluate the objective thermal comfort levels during experiments, predicted mean vote (PMV) computations (Fanger 1967). The PMV values were obtained using 2 min averages of M, W, T_{in}, RH_{in}, V, and T_{rad} responses recorded inside the experiment room during both exercise and resting periods, using the equations in BS EN ISO 7730 (ISO7730) using Center for Built Environment's Thermal Comfort Tool (Tartarini et al. 2020). Required clothing insulation (I_{cl}) values were determined to be 0.14 clo by the charts in ASHRAE's Thermal Comfort in Handbook of Fundamentals (ASHRAE 2009). The obtained PMV values are numbers between −3 and +3, which correspond to thermal sensation states depicted in ASHRAE's 7-point thermal sensation scale. Although the PMV method might lead to discrepancies from the genuine thermal perception during physical activity (Yang et al. 2020), it remains useful for facilitating easy comparisons across different thermal environments by estimating an individual's thermal sensation during exercise (Zora et al. 2017; Jia et al. 2022; Lian 2024).

A thermal sensation vote (TSV) questionnaire was conducted during the experiments for the subjective thermal comfort evaluation. The participants were asked to point their answer to the single question "What is your general thermal sensation?" every 2 minutes during exercise and resting periods (ASHRAE 2020; Pekdogan and Avci 2022). The answers were in the form of the 7-point thermal sensation scale. In this study, the TSV index is utilized for subjective thermal comfort evaluation, while the PMV index is used for objective evaluation.

It is important to note that while PMV is derived from physiological and environmental parameters, including metabolic heat production rate (M), external work rate (W), indoor air temperature (T_{in}), indoor relative humidity (RH_{in}), air velocity (V), and radiant temperature (T_{rad}), its inclusion alongside TSV is a common practice in thermal comfort studies (Zhou et al. 2022; Kramer et al. 2023). This convention allows for a comprehensive examination of thermal comfort conditions, considering both objective predictions and subjective perceptions (Zaniboni et al. 2020). Moreover, applying ensemble machine learning to both objective (PMV) and subjective (TSV) data enables a more robust analysis that captures the relationship between physiological responses and perceived thermal comfort sensations.

2.1.6 Refined dataset

Features influencing thermal comfort were selected under three categories: physiological responses, energy transfer modes, and environmental parameters. The independent variables included in the dataset of this study are as follows:

- Five variables of physiological responses: T_{sk}, T_{cr}, RH_{sk}, HR, and VO_2
- Five variables of energy transfer modes: C, R, E_{sk}, Q_{res}, $M–W$
- Four variables of environmental parameters: T_{in}, RH_{in}, V, and T_{rad}

The study's dependent variables consist of PMV and TSV, which represent the objective and subjective thermal comfort indices, respectively. All measured and computed variables were refined to 2 min averages during 30 min exercise and 20 min resting intervals. The dataset was compiled from data collected from seven participants with 25 observations each, resulting in a total of 175 observations.

2.2 Machine learning model construction

A comparative analysis was performed using the study's dataset to evaluate the performance of various machine learning regression algorithms, including multiple linear regression, decision tree regressor, random forest regressor, and support vector regressor. The aim was to select the model with the highest estimating capacity for PMV and TSV comfort indices. The evaluation criteria included mean squared Error (MSE), mean absolute error (MAE), and R-squared (R^2) score for four model sets, which are PMV-Exercise, PMV-Resting, TSV-Exercise, and TSV-Resting. Each sub-dataset was randomly divided into training and test sets in an 8/2 ratio, where 80% of the data was utilized for training and the remaining 20% for testing the models. The GBR was selected for this study, regarding the evaluation results of the four subsets. The performance results of each machine learning (ML) model are presented in Table A1 of Appendix, which is available in the Electronic Supplementary Material (ESM) of the online version of this paper.

As an ensemble learning model, GBR generates multiple weak learners (typically decision trees) sequentially to correct the preceding model's errors. GBR is well-suited for regression tasks and is known for its ability to handle complex relationships between features and target variables (Rao et al. 2019). It also provides robustness against overfitting, which is particularly important for small to medium-sized datasets like the one used in this study. GBR is a suitable model for thermal comfort studies due to its capability to handle complex relationships between features and target variables effectively in regression tasks, as indicated by previous studies (Rysanek et al. 2021; Morozova et al. 2022; Yang et al. 2022b).

In the context of this study, GBR optimizes a differentiable objective function through iterative adjustments guided

by the negative gradient direction (Friedman 2001). This process enhances the model by emphasizing misclassified or incorrectly predicted data points, near to gradient descent. Like other boosting models, GBR progressively refines a base model based on prior performance evaluations (Liu et al. 2022). According to that, the algorithm proceeds in the following steps:

- Initialization: The initial model is constructed, often a simple model like the mean of the target variable.
- Iterative Process: A series of weak models (usually decision trees) are added iteratively to the ensemble. Each new model is trained to correct the errors of the previous ensemble.
- Weighted Learning: The weak models are given weights based on their performance in the previous iteration. Models that significantly reduce errors are assigned higher weights.
- Combining Predictions: The predictions from all weak models are combined to create the final ensemble prediction.

Mathematically, the prediction from the ensemble model can be represented as in Equation (11) (Friedman 2001). In this general form, $F(\mathbf{x})$ represents the final prediction, J is the number of weak models, $f_j(\mathbf{x})$ is the prediction of the j^{th} weak model, and γ_j is a scaling factor assigned to the j^{th} model. This process was repeated for each PMV and TSV prediction during exercise and resting periods.

$$F(\mathbf{x}) = \sum_{j=1}^{J} \gamma_j f_j(\mathbf{x}) \tag{11}$$

2.2.1 Model performance assessment

In this study, three crucial performance assessment metrics of machine learning regression models were implemented, which are mean squared error (MSE), mean absolute error (MAE), and *R*-squared (R^2) (Barut and Bilgin 2023). These metrics quantify the predictive accuracy, the average magnitude of errors, and the fitting performance of the models, respectively (Guo et al. 2023). MSE refers to the average of the squared differences between predicted ($\tilde{y}_i$) and actual values (y_i), which is calculated as in Equation (12). In these equations, n represents the observation number in the dataset.

$$\mathrm{MSE} = \frac{1}{n}\sum_{i=1}^{n}(y_i - \tilde{y}_i)^2 \tag{12}$$

MAE signifies the average of the absolute differences between predicted ($\tilde{y}_i$) and actual values (y_i), which is calculated as in Equation (13).

$$\mathrm{MAE} = \frac{1}{n}\sum_{i=1}^{n}|y_i - \tilde{y}_i| \tag{13}$$

R^2 score, also addressed as the coefficient of determination assesses the proportion of the variance in the dependent variable that is explained by the independent variables. It is calculated as in Equation (14). In this equation $\overline{y}_i$ symbolizes the average of the actual values.

$$R^2 = 1 - \frac{\sum_{i=1}^{n}(y_i - \tilde{y}_i)^2}{\sum_{i=1}^{n}(y_i - \overline{y}_i)^2} \tag{14}$$

2.2.2 Hyperparameter tuning

Model performance optimization with hyperparameter tuning is an essential phase in machine learning model construction (Singh et al. 2023). In this study, the hyperparameter tuning process was executed using the GridSearchCV method from the sklearn.model_selection module in Python 3.11.3 to enhance the models' predictive performances (Pedregosa et al. 2011). This method explores various hyperparameter combinations to discover the configuration with the best outcomes for the PMV and TSV predictions during exercise and resting periods. The tuned hyperparameters contain:

- Number of Estimators that represent the number of weak models to be sequentially added to the ensemble,
- Learning Rate that governs the weight assigned to each weak model's contribution to the ensemble,
- Maximum Depth indicates the maximum depth of the individual decision trees, which impacts model complexity indirectly.

The optimization focused on minimizing the MSE values while enhancing the R^2 scores in this study's models. It was aimed to create a balance between model complexity and predictive performance. The final results reflected the power of the four GBR models in predicting thermal comfort indices.

2.2.3 Interpretation of feature importance analysis

The feature importance assessment is crucial in determining the contributions of different variables to the thermal comfort prediction (Chen et al. 2023). This analysis helps to comprehend the relationships among the considered physiological, energy transfer, and environmental parameters. Each feature's importance level is quantified as a percentage that represents its proportionate contribution to the overall predictive capacity of the GBR model. In this study, the feature importance analyses were done using the permutation feature importance technique. Permutation feature importance quantifies how a model's prediction

error changes when the values of a feature are randomly shuffled, disrupting its connection to the actual outcome (Motylinski et al. 2022). A feature is considered significant if altering its values raises prediction error, indicating its impact on the model's predictions. In contrast, a feature is deemed insignificant if shuffling its values maintains the same prediction error, implying the model's independence from that feature (Jing et al. 2023). In Breiman's work in 2001 (Breiman 2001), the evaluation of permutation feature importance is introduced for random forests. Building upon this idea, Fisher and colleagues (Fisher et al. 2019) introduced "model reliance", a feature importance approach that transcends specific models. The permutation future importance analysis steps are:

- The error of the base model ($\mathbf{e}_b$) is calculated as in Equation (15) using MSE. $\mathbf{X}$ symbolizes the feature matrix, and $\mathbf{y}$ is the equivalent target sequence, while L represents the loss or error function used in the evaluation of model performance.

$$\mathbf{e}_b = L\left(\mathbf{y}, \tilde{f}(\mathbf{X})\right) \tag{15}$$

- The feature $\mathbf{x}$ is rearranged within the dataset $\mathbf{X}$ to create a new feature matrix $\mathbf{X}_{perm}$, effectively disrupting the connection between feature $\mathbf{x}$ and the actual label $\mathbf{y}$.
- A new error estimate ($\mathbf{e}_p$) is calculated by utilizing the permuted feature matrix, which is derived from forecasts made on the permuted data, as in Equation (16).

$$\mathbf{e}_p = L\left(\mathbf{y}, \tilde{f}(\mathbf{X}_{perm})\right) \tag{16}$$

- The difference between permutated and base error gives the feature importance value $\mathbf{I}_x$ defined in Equation (17). Then, by dividing each permutation feature importance score by the sum of all scores and multiplying them by 100, the scores were presented in percentages.

$$\mathbf{I}_x = \mathbf{e}_p - \mathbf{e}_b \tag{17}$$

A lower or negative permutation feature importance score indicates that shuffling a specific feature had minimal impact or even improved the model's performance, suggesting that this feature holds lesser relevance for predicting the target variable (Antonopoulos et al. 2021). The feature importance analysis was conducted using the permutation_importance function from the sklearn.inspection module in Python 3.11.3 (Pedregosa et al. 2011).

3 Results

3.1 Descriptive data analysis

In this section, graphs of the variables, descriptive statistics, and correlation analysis are given for both the exercise and resting phases. The average T_{cr} and T_{sk} responses of the participants are presented in Figure 3. T_{cr} increased to 38 °C until the exercise period ended, then decreased to 37.5 °C until the 20th minute of the resting period. This indicates the residual heat stress gained during the exercise that could not be released from the body during the 20 min resting. Conversely, T_{sk} decreased from 27.9 °C to 26.8 °C until the 8th minute of the exercise period. After T_{sk} was recorded at 27.5 °C at the end of the exercise, it increased to 27.9 °C during the resting period.

The average skin relative humidity (RH_{sk}) of the participants and indoor relative humidity (RH_{in}) responses are presented in Figure 4. The average RH_{sk} increased from 35%±2% at the beginning of the exercise to 93%±2% in the 30th minute. As the exercise period ended, RH_{sk} decreased to 33%±1% by the end of the resting period. On the other hand, the average RH_{in} responses were kept at 42%±3% without a significant deviation during both exercise and resting periods.

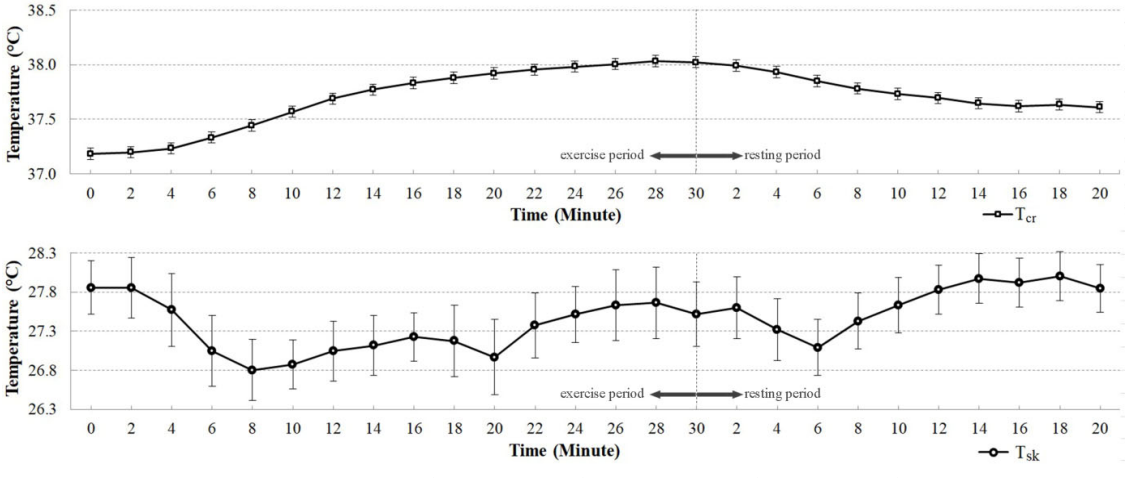

Fig. 3 Average T_{cr} and T_{sk} responses during exercise and resting periods

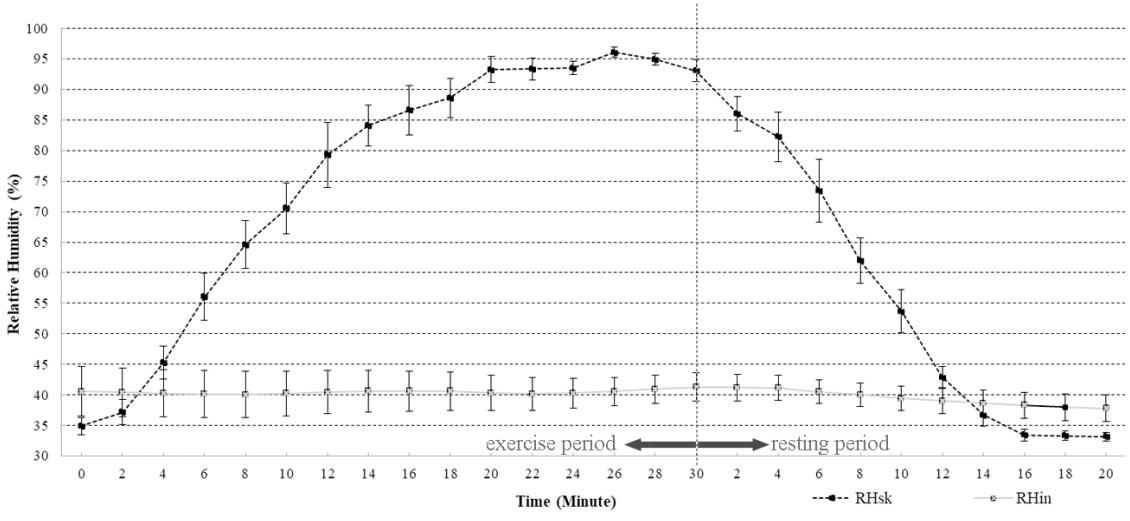

Fig. 4 Average RH_{sk} and RH_{in} responses during exercise and resting periods

The recorded averages of the net metabolic heat production rate ($M–W$), required heat storage rate (S), heat transfer rates through convection (C), radiation (R), evaporation (E_{sk}), and respiration (Q_{res}) of the participants are presented in Figure 5 for every 2 minutes of exercise and resting periods. $M–W$ recorded at 102±12 W/m^2 at the beginning of the exercise and increased to the range between 316±14 W/m^2 and 348±10 W/m^2 from the 4th minute until the end of the exercise. At the end of the resting period, $M–W$ decreased to 82±4 W/m^2. In order to release this heat gain to the environment, E_{sk}, C, R, and Q_{res} were employed as heat transfer agents during the exercise. The portion that could not be released immediately was stored inside the body, which was indicated as the area below the line of S in the graph.

Table 2 presents the descriptive statistics of the dataset, offering a summarized view of the central tendencies and dispersion of each factor across the two distinct periods. The statistics include means, standard deviations, minimums, maximums, and quartile values to understand the dataset's distribution comprehensively.

The correlations between the variables to understand potential relationships and dependencies were examined. Figure 6 shows the correlation matrices of each period, providing a visual representation of the strength and direction of associations between the factors for both the resting and exercise periods. Higher positive correlations (closer to 1) indicate a more robust direct relationship, while higher negative correlations (closer to −1) suggest an inverse relationship. Lower correlations imply weaker associations between variables. The p-values of the pair correlations for exercise and resting periods are presented in Table A2 and Table A3 in the ESM, respectively.

In the study, it was found that some correlations

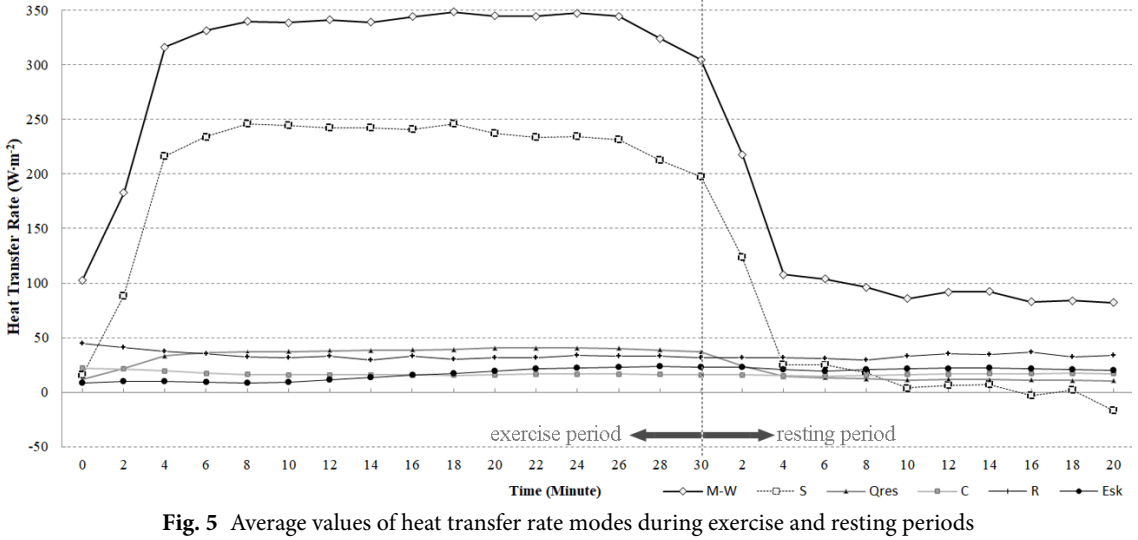

Fig. 5 Average values of heat transfer rate modes during exercise and resting periods

Table 2 Descriptive statistics of the dataset

Exercise period																
Factors	T_{sk} (°C)	T_{cr} (°C)	RH_{sk} (%)	HR (bpm)	VO_2 (mL/(kg·min))	C (W/m²)	R (W/m²)	E_{sk} (W/m²)	Q_{res} (W/m²)	$M-W$ (W/m²)	T_{in} (°C)	RH_{in} (%)	V (m/s)	T_{rad} (°C)	TSV	PMV
mean	27.3	37.7	78.4	131.7	37.1	16.8	33.2	15.8	37.2	326.8	21.2	42.9	0.15	21.4	1.10	0.75
std	1.06	0.40	20.2	25.88	6.07	3.66	7.02	7.08	6.23	56.30	1.05	10.9	0.07	1.08	1.05	0.63
min	24.9	36.7	28.3	59.57	10.3	9.51	18.3	5.18	14.6	99.50	18.6	27.8	0.07	18.8	−1.00	−1.90
25%	26.4	37.5	67.1	115.4	34.4	14.4	28.1	9.59	34.7	313.2	20.7	34.1	0.11	20.7	0.00	0.64
median	27.2	37.7	87.2	134.3	37.6	16.6	32.9	13.9	37.6	337.6	21.0	37.4	0.14	21.2	1.00	0.71
75%	28.0	37.9	95.1	151.9	41.6	19.4	37.0	21.6	41.4	361.0	21.8	52.9	0.17	21.9	2.00	1.15
max	29.7	38.6	99.2	170.1	45.8	27.8	54.4	32.6	46.8	393.7	23.9	64.0	0.66	24.5	3.00	1.82
Resting period																
Factors	T_{sk} (°C)	T_{cr} (°C)	RH_{sk} (%)	HR (bpm)	VO_2 (mL/(kg·min))	C (W/m²)	R (W/m²)	E_{sk} (W/m²)	Q_{res} (W/m²)	$M-W$ (W/m²)	T_{in} (°C)	RH_{in} (%)	V (m/s)	T_{rad} (°C)	TSV	PMV
mean	27.7	37.7	53.7	95.80	9.77	16.3	32.9	21.1	13.2	104.4	22.0	41.0	0.11	21.9	0.03	−1.50
std	0.90	0.33	21.3	14.03	3.85	4.02	8.34	5.81	4.44	44.45	0.98	8.1	0.04	1.24	0.72	1.05
min	25.1	37.3	29.9	75.50	5.88	8.32	10.8	7.76	8.89	65.66	20.6	28.8	0.05	19.7	−1.00	−3.00
25%	27.3	37.5	35.2	85.31	7.93	13.7	28.1	18.6	10.8	84.63	21.3	34.5	0.08	21.3	0.00	−2.20
median	27.8	37.7	44.3	91.88	8.85	15.9	34.9	20.7	12.1	92.00	21.7	38.8	0.10	21.5	0.00	−1.67
75%	28.3	37.9	72.7	103.7	9.95	19.1	37.8	25.3	13.6	104.0	23.1	48.9	0.14	22.7	0.00	−1.14
max	29.0	38.6	94.2	140.3	26.2	24.9	47.8	33.2	31.6	277.7	23.9	54.6	0.21	25.9	2.00	1.82

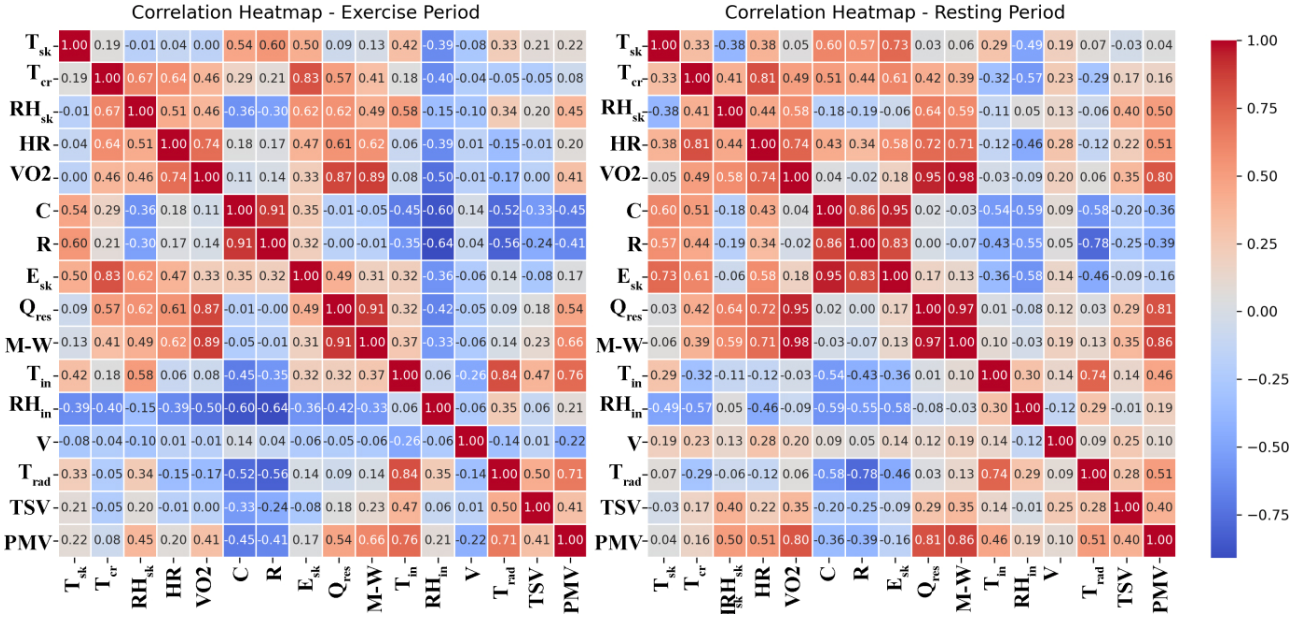

Fig. 6 Correlation heatmaps for each period of the study

between the analyzed variables exhibit high levels of multicollinearity. Based on the threshold of 0.75 for multicollinearity analysis, pairs of variables exhibiting high correlation are presented in Table 3. Although multicollinearity typically requires treatment in GBR models, in this study, all factors were included regardless. This decision is justified for several reasons. Firstly, the study primarily focuses on the TSV dependent variable, which remains uncorrelated with any other variable. Secondly, while collinearity was expected between some variables used to calculate PMV, including collinear factors ensures integrity between PMV and TSV variables for comparison. Moreover, despite the high correlations among variables related to the modes of human body energy transfer rates (C, R, E_{sk}, Q_{res}, and $M–W$), including them separately allows for a comprehensive analysis of their relationship with

Table 3 Pairs with multicollinearity

Exercise dataset			Resting dataset		
Q_{res}	VO_2	0.87	Q_{res}	VO_2	0.95
$M-W$	VO_2	0.89	$M-W$	VO_2	0.98
R	C	0.91	R	C	0.86
$M-W$	Q_{res}	0.91	$M-W$	Q_{res}	0.97
T_{rad}	T_{in}	0.84	E_{sk}	C	0.95
PMV	T_{in}	0.76	E_{sk}	R	0.83
			T_{rad}	R	−0.78
			HR	T_{cr}	0.81
			PMV	VO_2	0.80
			PMV	Q_{res}	0.81
			PMV	$M-W$	0.86

thermal comfort. With this acknowledgment of the presence of multicollinearity, additional analyses were conducted to elucidate the factors influencing the phenomenon under investigation.

3.2 Thermal comfort indices during exercise and resting periods

The results of the thermal comfort responses are presented in Figure 7 according to the recorded minutes during the exercise and resting period. It visualizes the variations in predicted mean vote (PMV) values, thermal sensation vote (TSV) responses for each participant, and the averages within 2 min intervals. In both the exercise and resting phases, distinctive patterns were seen for PMV and TSV. Notably, both indices demonstrate a gradual descending trend that indicates a shift from warmer sensations during exercise to cooler sensations during resting as time progresses. The data indicated a moderate fit of the PMV responses (R^2: 0.47) to the regression line, while the fit for TSV responses (R^2: 0.2) yields weaker. In the early stages of exercise, specifically at the 2nd minute, participants reported a mean TSV of 0.29 with a standard deviation of 0.49, which implies an initial perception of warmth. Conversely, the mean PMV at the same time was below zero, recorded at −0.49 with a standard deviation of 0.73, indicating a perceived cooler sensation. However, beginning with the 6th minute of exercise, a divergence in responses becomes evident as the mean PMV value is 0.87 with a standard deviation of 0.53. In contrast, TSV responses showed a broader distribution with a mean of 1.20 and a standard deviation of 1.08 until the 30th minute. This divergence suggests that, despite objective assessments reflecting a lower mean PMV range, participants experienced varying thermal sensations, highlighting the subjectivity of thermal comfort perception.

As for the resting period, although both PMV and TSV responses exhibit a decline toward colder sensations, TSV responses tend to be closer to neutral sensations, with a mean of 0.03 and a standard deviation of 0.72. Meanwhile, the average PMV responses during the resting period indicate a consistent perception of cold, with a mean PMV of −1.50 and a standard deviation of 1.06. This contrast suggests that while the environment's objective evaluation indicates a colder sensation during the resting period, the subjective thermal sensation responses are comparatively milder, with the majority reporting closer to neutral sensation.

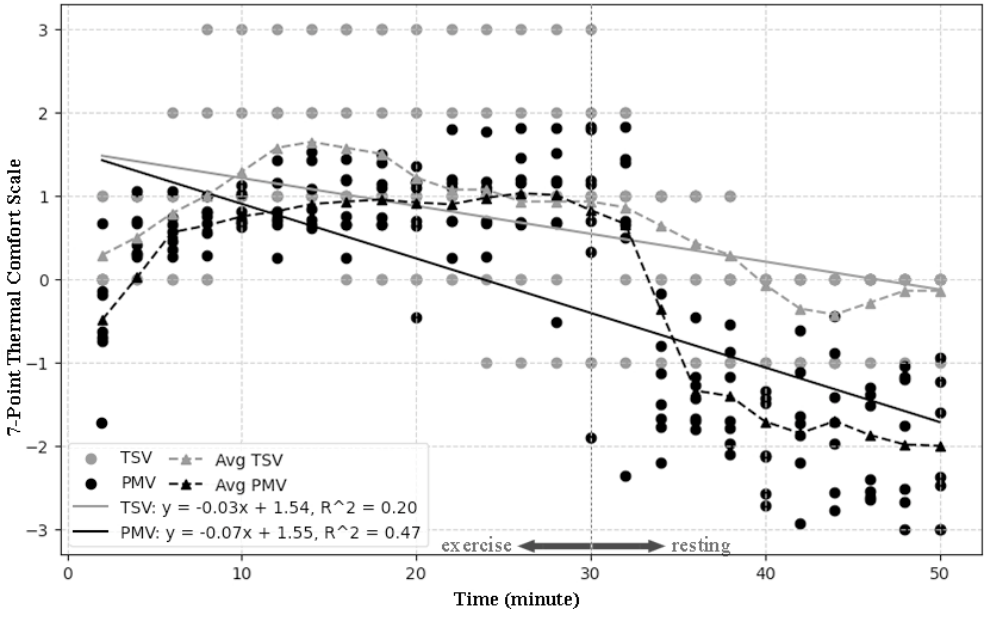

Fig. 7 Scatter plot of PMV and TSV based on time of the exercise and resting periods

The presented scatter plot in Figure 8 reveals the relationship between thermal comfort indices and the net metabolic heat production rate ($M–W$). Notably, TSV and PMV responses showcase distinct trends across varying levels of $M–W$, which refers to the shifts in subjective and objective thermal comfort perceptions. The trend line for PMV (R^2: 0.82) indicates a stronger linear relationship between PMV and $M–W$ during the exercise and resting periods. In contrast, the TSV regression line (R^2: 0.3) shows a milder relationship, which suggests subjective responses are less affected by $M–W$ during exercise and resting. When $M–W$ is lower (50–150 W/m^2), TSV values tend to cluster around a more neutral sensation range between −1 and 1 (mean TSV: 0.58, std: 1.06), while PMV values suggest colder sensations within the range of 0 to −3 (mean PMV: −0.38, std: 1.48). This divergence between TSV and PMV responses underscores the complexity of the thermal comfort experience, wherein participants tend to feel more neutral, although objective predictions cooler sensation vote.

3.3 Performance of the gradient boosting regressor (GBR) models

The performance evaluation of the developed GBR models provides insights into their predictive capabilities of thermal comfort using mean squared error (MSE), mean absolute error (MAE), and R^2 indices. Table 4 summarizes the performance indices of the models for both PMV and TSV predictions during exercise and resting periods.

Table 4 Performance indices of the developed GBR models

Indices	PMV-Exercise	PMV-Resting	TSV-Exercise	TSV-Resting
MSE	0.07	0.13	0.49	0.12
MAE	0.16	0.23	0.52	0.23
R^2	0.69	0.87	0.25	0.76

The PMV-Exercise model demonstrates promising predictive accuracy, with an MSE of 0.07, indicating a relatively small squared difference between predicted and actual values. The MAE of 0.16 suggests a moderate absolute difference, while the R^2 score of 0.69 signifies that the model captures approximately 69% of the variance in the data. Comparatively, the PMV-Resting model showcases even better performance with an MSE of 0.13 and an MAE of 0.23, which refers to a higher accuracy in predicting PMV during the resting period. The R^2 score of 0.87 implies that the model effectively explains about 87% of the variance during resting periods.

On the other hand, the TSV-Exercise model presents some challenges in prediction accuracy. The relatively high MSE of 0.49 indicates less accurate predictions and a higher MAE of 0.52. Moreover, the low R^2 score of 0.25 suggests that this model struggles to capture the variation in TSV during exercise. In contrast, the TSV-Resting model exhibits an improved performance with an MSE of 0.12 and a consistent MAE of 0.23. It provides more accurate predictions for TSV during resting periods. The R^2 score of 0.76 highlights the model's ability to explain a substantial

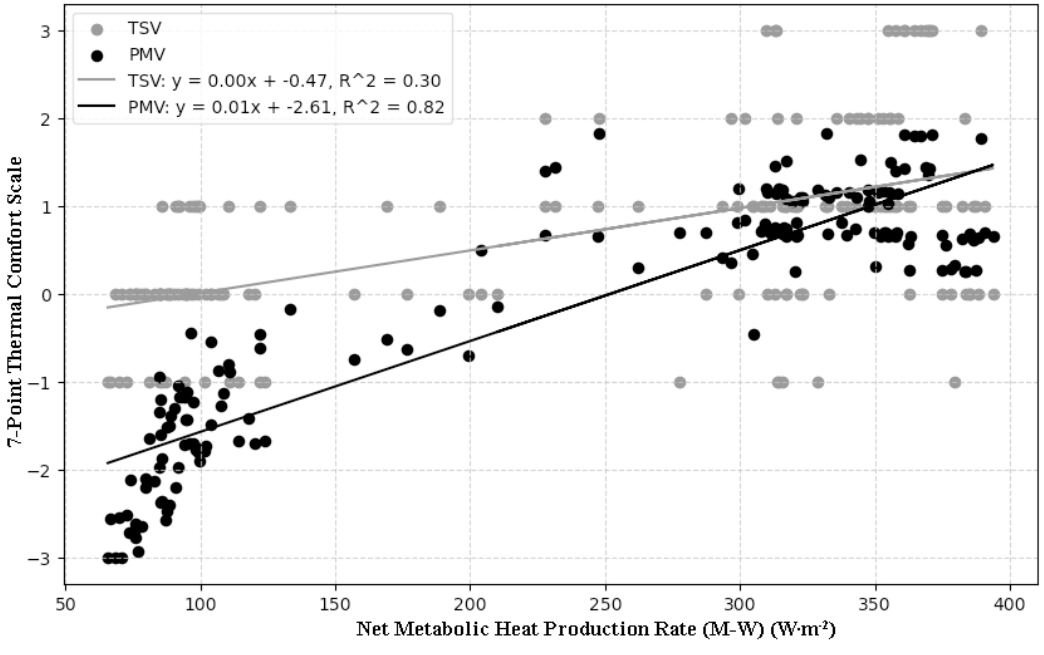

Fig. 8 Scatter plot of PMV and TSV based on $M–W$ during exercise and resting periods

portion of the variance during rest. Comparing all the models, the models predicting PMV during exercise and resting outperform the models of TSV, specifically during exercise.

Figure 9 provides a summary of the statistics for the residuals of each model. The residuals represent the differences between the predicted and actual values of the thermal comfort indices. The distribution of the residuals provides information on the accuracy of the model predictions. Lower values of standard deviation (σ) indicate that the model's predictions are closer to the actual values, while higher values suggest greater variability. As for the mean (μ) of the residuals, a value close to zero indicates that the model's predictions are closer to accuracy. A negative mean indicates that the model tends to overpredict, while a positive mean suggests underprediction. Comparing the four models, the PMV-Exercise model has the lowest standard deviation, indicating consistent and precise predictions during exercise periods. Conversely, the TSV-Resting model exhibits a higher standard deviation, implying greater prediction variability during resting periods. Regarding the mean, the TSV Resting model has a substantial negative value, suggesting a consistent tendency to overpredict during resting periods.

3.4 Feature importance analysis

In the context of thermal comfort prediction, a feature importance analysis was performed to unravel the complex relationship of physiological, heat transfer, and environmental factors for exercise and resting scenarios. The feature importance analysis unveils the relative significance of factors in shaping thermal comfort predictions, with each percentage representing a factor's contribution to the model's predictive capability. Figure 10 presents each model's permutation feature importance analysis results in percentages. For the PMV-Exercise model, factors such as T_{rad} and $M–W$ emerge as primary drivers, accounting for approximately 53.4% and 32.6% of the predictive capacity, respectively. Meanwhile, the PMV Resting model places considerable emphasis on $M–W$ and T_{rad}, contributing around 55.0% and 25.7%, respectively. Shifting to the TSV-Exercise model, a notable factor is E_{sk}, standing out with an importance of 51.0%. Furthermore, the TSV-Resting model highlights the significance of T_{cr} and time, which contribute approximately 36.1% and 29.7%, respectively. Considering the average of all the models, $M–W$ remains an integral factor with an average importance of 24.2%, followed closely by T_{rad} at 17% and E_{sk} at 13.1%.

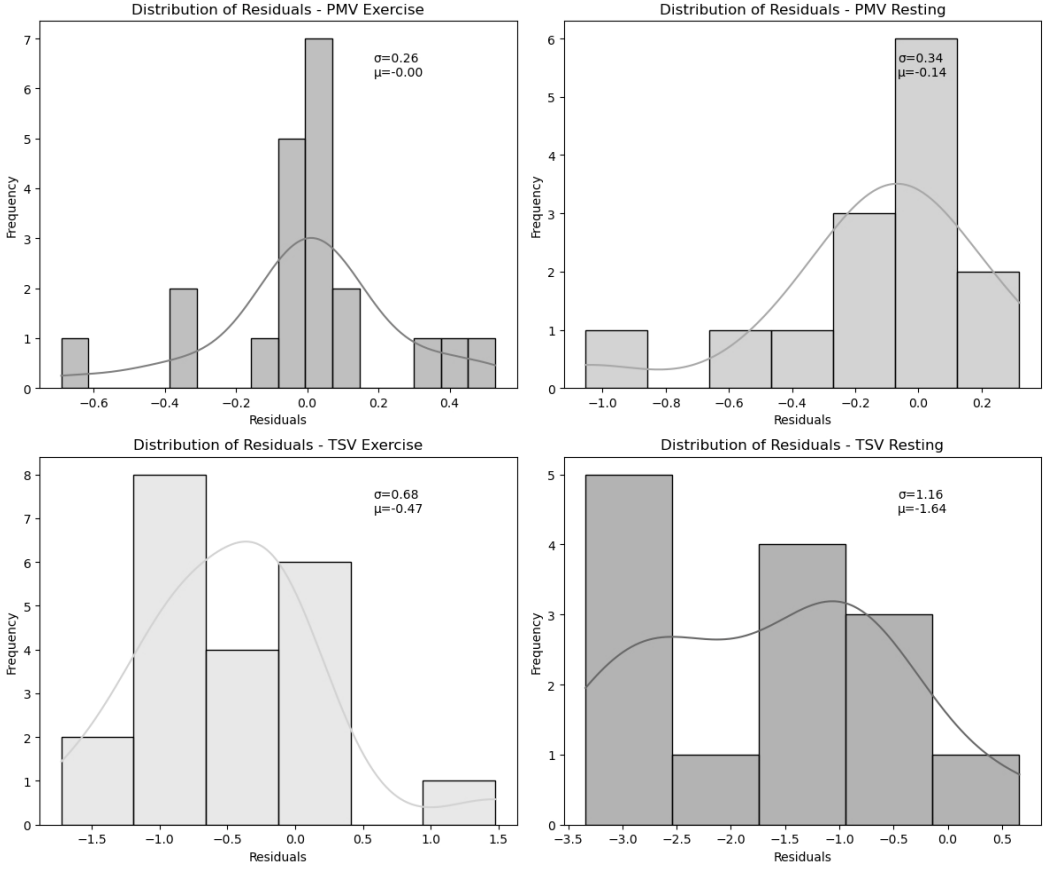

Fig. 9 The distribution of prediction residuals by the GBR models

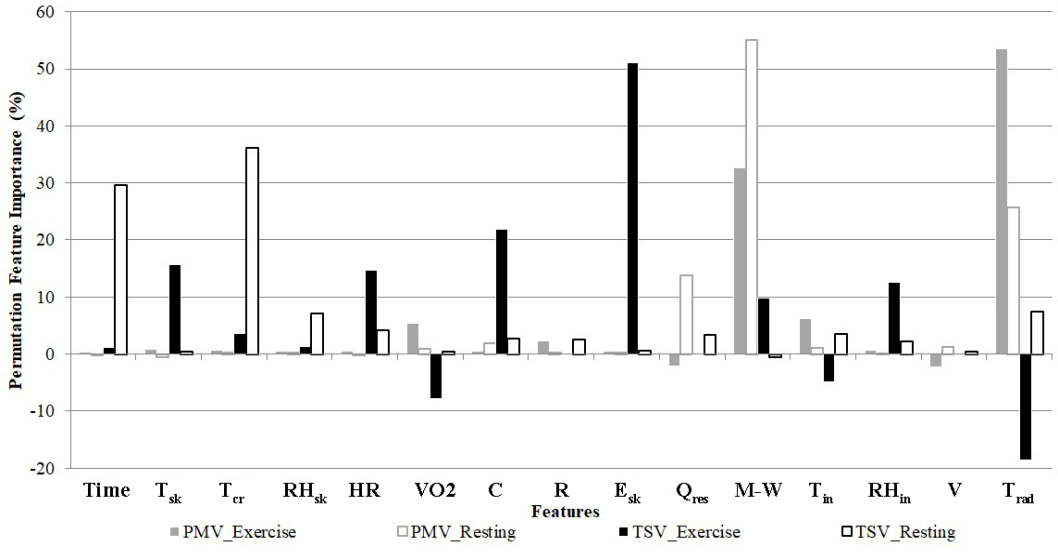

Fig. 10 Feature importance analysis results of each model

4 Discussion

The present study investigated the relationship among physiological responses, heat transfer modes, and environmental factors on subjective and objective thermal comfort perceptions during exercise and resting. The findings revealed through descriptive data analysis, correlation analysis, and predictive modeling reported on the complex nature of human thermal comfort perception. They provided insights into the design and management of indoor environments.

4.1 Impact of physiological responses, heat transfer modes, and environmental factors

The descriptive data analysis showed distinct physiological and environmental variable patterns across exercise and resting phases. T_{cr} and T_{sk} responses exhibited intriguing dynamics, revealing how the body adapts to changes in thermal load. During exercise, T_{cr} exhibited a steady increase, reaching its peak towards the end of the exercise. At the same time, T_{sk} displayed a decrease initially and then subsequently returned to pre-exercise levels during resting (Figure 3). The decrease in the T_{sk} responses in the early stages of the exercise is attributed to the escalated cutaneous sympathetic vasoconstrictor outflow that prevents the skin blood flow until T_{cr} reaches around 37.2 °C (Kenney and Johnson 1992). This divergence emphasized the intricate balance between core and skin temperature, underlining the complexity of thermoregulation during exercise (Liu et al. 2021; Simmons et al. 2011).

The strong correlation between M–W and PMV highlights the significance of metabolic heat production in shaping objective thermal comfort evaluation. The observation that increasing activity rate is a significant determinant of PMV during exercise and resting periods is consistent with previous research (Zhai et al. 2020; Zhang et al. 2020a). Additionally, the trends observed in the relationships between RH_{sk} and RH_{in} reveal the dynamic interplay involving the minute of observation and skin relative humidity during exercise and resting periods. These findings contribute to understanding how evaporative heat transfer is utilized, particularly in the transition between the exercise and resting periods. However, the complex interaction of physiological responses and thermal comfort perception indicates the multifaceted relationship that the GBR models developed in the study aim to capture.

4.2 Thermal comfort perception: Objective vs. Subjective

The findings revealed a consistent trend transitioning from warmer sensations during exercise phase to cooler sensations during resting period as time progressed. This pattern was objectively captured by the moderate fit of PMV responses (R^2: 0.47) to the regression line, indicating a credible alignment between predicted and observed thermal sensations. Conversely, TSV responses demonstrated a weaker fit (R^2: 0.2), suggesting a more diverse and nuanced subjective experience that cannot be solely explained by objective metrics (Lin et al. 2023).

A divergence between PMV and TSV responses emerged as exercise duration increased. Although the mean PMV values indicated a cooler thermal sensation (mean: 0.87, std: 0.53) compared to the beginning of the exercise, TSV responses showed a broader distribution (mean: 1.20, std: 1.08) until the 30th minute. This divergence emphasized

the subjective nature of thermal comfort perception, where participants' individual experiences exhibited wider variability compared to the objective PMV assessments. This finding aligns with previous research that emphasizes the intricate relationship between physiological responses and individual perceptions (Mou et al. 2022).

Both PMV and TSV responses declined towards colder sensations during the resting period. Notably, TSV responses tended to converge closer to neutral sensations (mean: 0.03, std: 0.72), while average PMV responses indicated a consistent perception of cold (mean: −1.50, std: 1.06). This divergence in the subjective and objective evaluations during the resting phase highlights the intriguing dynamics of human thermal perception (Vellei et al. 2021). While the environment's objective evaluation pointed to a colder sensation, individuals' subjective experiences were comparatively milder, with the majority reporting sensations closer to neutrality.

As for the relationship between thermal comfort indices and net metabolic heat production rate (M–W), the PMV responses demonstrated a robust linear relationship with M–W (R^2: 0.82), suggesting that metabolic heat production significantly influences perceived thermal comfort. In contrast, the TSV responses exhibited a milder linear relationship (R^2: 0.3), indicating that M–W less influenced subjective thermal sensations during exercise and resting. Furthermore, lower M–W levels (50–150 W/m^2) prompted TSV values to cluster around a more neutral sensation range (mean: 0.58, std: 1.06), while PMV values indicated colder sensations within the range of 0 to −3 (mean: −0.38, std: 1.48). This divergence highlights the difference between objective predictions and subjective experiences, where participants tended to perceive more neutral sensations despite the PMV predicting cooler thermal sensations (Zhang et al. 2020b).

4.3 GBR models' performances

The PMV-Exercise GBR model stands out with its promising predictive accuracy with an MSE of 0.07, which indicates a relatively small squared difference between predicted and actual values, emphasizing the model's capability to approximate thermal sensations during exercise. The corresponding MAE of 0.16 reveals a moderate absolute difference, while the R^2 score of 0.69 signifies that the model captures around 69% of the variance in the data. The PMV-Resting GBR model, on the other hand, exhibits better performance with an MSE of 0.13 and an MAE of 0.23. This higher accuracy in predicting PMV during rest is supported by the R^2 score of 0.87, indicating that the PMV-Resting Model effectively explains 87% of the variance during resting.

Conversely, the TSV-Exercise GBR model showed challenges in prediction accuracy with higher MSE of 0.49 and MAE of 0.52. The low R^2 score of 0.25 indicates the TSV-Exercise Model's inability to capture the variations of TSV responses during exercise. In contrast, the TSV-Resting GBR model performed better, with an MSE of 0.12 and a MAE of 0.23. These results collectively strengthen the GBR model's ability to predict TSV during resting periods, as indicated by the R^2 score of 0.76, which implies that the model explains a substantial portion of the variance during rest. The comparison of all the GBR models shows that those predicting PMV during exercise and resting period surpass the models for TSV, particularly during exercise.

As for the distribution of prediction residuals by the GBR models, the PMV-Exercise model boasts the lowest standard deviation, indicating consistent and precise predictions during exercise. Resting model exhibits a higher standard deviation, implying greater prediction variability during rest. The TSV Resting model's substantial negative mean brings about consistent overprediction during resting periods.

4.4 Feature importance

The results of the permutation feature importance analysis provide a nuanced view of each model's predictive capacity. The PMV-Exercise model highlights T_{rad} and M–W as primary drivers, contributing around 53.4% and 32.6% of the predictive capability, respectively. The prominence of M–W and T_{rad} in the PMV-Resting model, contributing approximately 55.0% and 25.7%, respectively, reaffirms the importance of metabolic heat production and radiant temperature in shaping objective comfort evaluation. As for the TSV-Exercise model, E_{sk} emerges as a significant factor with an importance level of 51.0%, which suggests the influence of local heat dissipation through evaporation during physical activity in subjective thermal comfort perception, aligning with prior research (Zhang et al. 2020c). Furthermore, the TSV-Resting model underscores the importance of T_{cr} and time, contributing around 36.1% and 29.7%, respectively, in shaping thermal comfort during rest.

Considering the average importance across all models, M–W maintains a central role with an average importance of 24.2%, followed by T_{rad} at 17.0% and E_{sk} at 13.1%. These findings indicate the complex nature of thermal comfort perception, where diverse physiological and environmental factor relationships need to be considered. Notably, the

emergence of radiant temperature as a significant feature in the PMV-Exercise model introduces a new dimension given that radiant temperature has often been disregarded, being assumed to be equal to the room temperature in thermal comfort studies (Fletcher et al. 2020). Moreover, these results emphasize the importance of heat transfer modes from the body in influencing thermal comfort conditions. Mechanical system designs that can provide varied environmental conditions based on different exercise and resting situations, along with correct positioning to facilitate effective heat transfer without causing discomfort, become crucial aspects in optimizing indoor environments for thermal comfort.

5 Limitations and future directions

While this study contributes to the understanding of thermal comfort perception during exercise and rest, it is noteworthy to mention the limitations. Although employing small participant numbers in cycling exercise studies is not uncommon in the literature (Hill and Smith 1999; Cannon et al. 2011;Ramirez-Campillo et al. 2018; Marko et al. 2022; Weavil et al. 2022) aimed at identifying different variables, it is essential to acknowledge that generalizations to broader populations should be approached cautiously. Additionally, the study focused solely on male participants, potentially limiting the application of findings to diverse demographic groups. To strengthen the robustness of future findings, it is recommended that subsequent studies involve more extensive and diverse samples. Furthermore, while the finding aligns with the interactions within human body thermoregulation, additional research is necessary to validate and contextualize these outcomes across a broader array of settings and diverse populations.

Moving forward from this study, future research can focus on assessing the effectiveness of personalized thermal comfort control systems in indoor exercise spaces. Guided by the outcomes gained from the predictive models developed in this study, future investigations can design and implement adaptive HVAC systems that match environmental conditions to individual preferences and activity levels. Integrating real-time physiological and environmental monitoring with machine learning algorithms can enable dynamic adjustments of temperature, humidity, and airflow to optimize thermal comfort during exercise and resting periods. Additionally, investigating the potential synergies between thermal comfort optimization and energy efficiency in indoor exercise facilities can lead to the development of innovative strategies for reducing environmental impact while enhancing user comfort and satisfaction. By addressing these research gaps, future studies can contribute to the advancement of knowledge and practice in the design and management of indoor exercise environments, ultimately providing healthier and comfortable indoor exercise experiences.

6 Conclusions

This study examined the relationship among physiological responses, heat transfer modes, and environmental factors on objective and subjective thermal comfort perceptions during exercise and resting periods. The investigation focused on the dynamics through descriptive data analysis, correlation analysis, and predictive modeling, thereby uncovering the multifaceted nature of human thermal comfort perception and producing knowledge for indoor physical exercise environments. The study's primary outcomes can be summarized as follows:

- A shift from warmer sensations during exercise to cooler sensations during resting phase was observed under the constant environmental conditions maintained throughout the experiments. The divergence between PMV and TSV responses emphasized the individualistic nature of thermal comfort perception, where personal experiences exhibited wider variability than objective metrics. The relationship between thermal comfort indices and net metabolic heat production rate ($M–W$) revealed the complexity of participants' experiences, where TSV trended toward neutrality while PMV predicted cooler sensations.
- The predictive models demonstrated varying performance across different conditions. The PMV-Exercise model showed accuracy during exercise, while the PMV-Resting model better predicted PMV values during the resting period. The TSV-Exercise model faced challenges in accurately predicting TSV during exercise, while the TSV-Resting model performed well during rest.
- The feature importance analysis of the PMV models during exercise and resting emphasized metabolic heat production and radiant temperature's (T_{rad}) role in shaping objective thermal comfort. The TSV-Exercise model identified the influence of local heat dissipation through evaporation during exercise (E_{sk}) as a significant factor. Similarly, the TSV-Resting model emphasized core temperature (T_{cr}) and observation time in shaping thermal comfort during rest.

In light of the study's findings, gyms can refine their indoor environmental parameters to optimize users' thermal comfort. Given the significant influence of T_{rad} on thermal comfort, gyms may consider employing radiant heating or cooling systems for precise T_{rad} control, thereby tailoring the environment to preferences of users. In addition, lower

heat transfer rates will contribute to T_{rad} to be closer to indoor air temperature levels, resulting in lower energy consumption rates. While temperature, air velocity, and relative humidity may not rank as primary drivers in the feature importance analysis, their regulation remains crucial due to their impact on heat transfer rates. The results emphasize a nuanced relationship between heat transfer rates and participants' thermal comfort perceptions. Gyms could install temperature, humidity and CO_2 control systems that adapt to users' activity levels, ensuring consistent comfort throughout workouts. Moreover, managing air velocity to facilitate efficient heat dissipation without discomfort, especially during exercise, is paramount. By integrating these adjustments informed by the study's results, exercise spaces can optimize indoor environments to enhance users' well-being and thermal comfort experience.

In addition to refining indoor environmental parameters based on the study's findings, the predictive power of the developed models in this study offers the potential to be used in indoor exercise spaces. With the PMV and TSV prediction models exhibiting varying degrees of accuracy and performance, gyms and fitness centers can utilize these models to adjust their HVAC systems to control the indoor environment more precisely. For instance, the PMV-Exercise and PMV-Resting models, which showed promising accuracy in predicting thermal sensations during exercise and resting periods, respectively, can inform HVAC system adjustments to maintain optimal comfort levels throughout different activity phases. By integrating these predictive models into HVAC control systems, gyms can dynamically adjust temperature, humidity, and airflow based on users' activities, enhancing overall comfort and well-being.

This study marks an initial step in utilizing machine learning to decipher the complex dynamics of thermal comfort perception in indoor exercise spaces. By unraveling the relationships among physiological responses, heat transfer modes, and environmental factors, this investigation provides a foundation for future research in the domain. The findings emphasize the importance of considering exercise and resting periods in indoor thermal comfort evaluation. Moreover, the study illuminates the essential role of heat transfer modes in shaping thermal comfort. This highlights the importance of including mechanical systems that can easily adjust to varying environmental demands during different activities. These results have significant implications for the design and maintenance of indoor exercise spaces, with the goal of providing spaces that foster optimal well-being and thermal comfort for individuals.

Electronic Supplementary Material (ESM): the appendix is available in the online version of this article at https://doi.org/10.1007/s12273-024-1142-5.

Acknowledgements

This work was supported by the Scientific and Technological Research Council of Türkiye (TÜBİTAK) Foundation under grant number 122M883.

Funding note: Open access funding provided by the Scientific and Technological Research Council of Türkiye (TÜBİTAK).

Declaration of competing interest

The authors have no competing interests to declare that are relevant to the content of this article.

Ethical approval

All the procedures conducted in the study were approved by the Ethics Committee for Medical Research of Medical School of Ege University with the report number 22-9.1T/20.

Declaration of generative AI and AI-assisted technologies in the writing process

During the preparation of this work the authors used Grammarly AI Writing Assistant in order to improve language and readability. After using this tool/service, the authors reviewed and edited the content as needed and take full responsibility for the content of the publication.

Author contribution statement

All authors contributed to the study conception and design. Material preparation, data collection and analysis were performed by Ali Berkay Avci, Görkem Aybars Balci, and Tahsin Basaran. The first draft of the manuscript was written by Ali Berkay Avci and all authors commented on previous versions of the manuscript. All authors read and approved the final manuscript.

References

Amaripadath D, Rahif R, Velickovic M, et al. (2023). A systematic review on role of humidity as an indoor thermal comfort parameter in humid climates. *Journal of Building Engineering*, 68: 106039.

Antonopoulos I, Robu V, Couraud B, et al. (2021). Data-driven modelling of energy demand response behaviour based on a large-scale residential trial. *Energy and AI*, 4: 100071.

ASHRAE (2009). Thermal comfort. In: Handbook Fundamentals. pp. 9.1–9.30.

ASHRAE (2020). ANSI/ASHRAE Standard 55–2020 Thermal Environmental Conditions for Human Occupancy. Atlanta, GA, USA: American Society of Heating, Ventilating and Air-Conditioning Engineers.

Avci AB, Balci GA, Basaran T (2024). Optimizing thermal comfort in physical exercise spaces: A study of spatial and thermal factors. *Energy and Buildings*, 303: 113782.

Balci GA, Basaran T, Colakoglu M (2016). Analysing visual pattern of skin temperature during submaximal and maximal exercises. *Infrared Physics & Technology*, 74: 57–62.

Balci GA, Avci AB, Colakoglu M, et al. (2024). Estimation of heat production rate using thermal data during exercise in indoor environments: A study of heat storage rate in male athletes. *International Journal of Biometeorology*, 68: 1109–1122.

Barut Z, Bilgin TT (2023). Applied comparison of polynomial regression and artificial neural networks methods for prediction of house prices. *Süleyman Demirel University Journal of Natural and Applied Sciences*, 27(1): 152–59. https://doi.org/10.19113/sdufenbed.1190150.

Breiman L (2001). Random Forests. *Machine Learning*, 45: 5–32.

Cannon DT, White AC, Andriano MF, et al. (2011). Skeletal muscle fatigue precedes the slow component of oxygen uptake kinetics during exercise in humans. *The Journal of Physiology*, 589: 727–739.

Chen G, Hua J, Shi Y, et al. (2023). Constructing air temperature and relative humidity-based hourly thermal comfort dataset for a high-density city using machine learning. *Urban Climate*, 47: 101400.

Cui Y, Fan C, Zhou X, et al. (2024). Factor analysis and risk assessment of indoor environmental parameters and TSV in fitness centres under different zones, exercise intensities and times. *Indoor and Built Environment*, https://doi.org/10.1177/1420326X241232116.

Deloitte (2022). European Health & Fitness Market Report. Available at https://www2.deloitte.com/content/dam/Deloitte/de/Documents/consumer-business/EHFMR_2022_Auszug_Report.pdf.

Du Bois D, Du Bois EF (1916). CLINICAL CALORIMETRY: TENTH PAPER A formula to estimate the approximate surface area if height and weight be known. *Archives of Internal Medicine*, https://doi.org/10.1001/archinte.1916.00080130010002.

Fanger P (1970). Thermal comfort: Analysis and applications in environmental engineering. Available at https://books.google.com.tr/books/about/Thermal_Comfort.html?id=S0FSAAAAMAAJ&redir_esc=y.

Fanger PO (1967). Calculation of thermal comfort-introduction of a basic comfort equation. *ASHRAE Transacions*, 73.

Fisher A, Rudin C, Dominici F (2019). All models are wrong, but many are useful: Learning a variable's importance by studying an entire class of prediction models simultaneously. *Journal of Machine Learning Research*, 20: 177.

Fletcher MJ, Glew DW, Hardy A, et al. (2020). A modified approach to metabolic rate determination for thermal comfort prediction during high metabolic rate activities. *Building and Environment*, 185: 107302.

Friedman JH (2001). Greedy function approximation: A gradient boosting machine. *The Annals of Statistics*, 29: 1189–1232.

Gao Y, Gao Y, Shao Z, et al. (2023). The effects of indoor temperature and exercise behavior on thermal comfort in cold region: A field study on Xi'an, China. *Energy*, 273: 127258.

Guo J, Yun S, Meng Y, et al. (2023). Prediction of heating and cooling loads based on light gradient boosting machine algorithms. *Building and Environment*, 236: 110252.

Hill DW, Smith JC (1999). Determination of critical power by pulmonary gas exchange. *Canadian Journal of Applied Physiology*, 24: 74–86.

Huang C, Que J, Liu Q, et al. (2021). On the Gym Air Temperature Supporting Exercise and Comfort. *Building and Environment*, 206: 108313.

Huang X, Zhang Q, Wang Z, et al. (2022). Thermal sensation under high-intensive exercise in naturally ventilated gymnasiums in hot-humid areas of China: Taking basketball players for example. *Indoor and Built Environment*, 31: 139–154.

ISO7730 (2005). BS.EN.ISO7730. Ergonomics of the Thermal Environment. Analytical Determination and Interpretation of Thermal Comfort Using Calculation of the PMV and PPD Indices and Local Thermal Comfort Criteria. International Organization for Standardization.

Jia X, Wang J, Zhu Y, et al. (2022). Climate chamber study on thermal comfort of walking passengers at different moving speeds. *Building and Environment*, 224: 109540.

Jia X, Li S, Zhu Y, et al. (2023). Transient thermal comfort and physiological responses following a step change in activity status under summer indoor environments. *Energy and Buildings*, 285: 112918.

Jing H, He X, Tian Y, et al. (2023). Comparison and interpretation of data-driven models for simulating site-specific human-impacted groundwater dynamics in the North China Plain. *Journal of Hydrology*, 616: 128751.

Kapalo P, Vojtasko L, Vasilisin D, et al. (2021). Investigation of the influence of the level of physical activity on the air exchange requirements for a gym. *Building and Environment*, 204: 108123.

Kenney WL, Johnson JM (1992). Control of skin blood flow during exercise. *Medicine and Science in Sports and Exercise*, 24: 303–312.

Kenny GP, Webb P, Ducharme MB, et al. (2008). Calorimetric measurement of postexercise net heat loss and residual body heat storage. *Medicine and Science in Sports and Exercise*, 40: 1629–1636.

Kenny GP, McGinn R (2017). Restoration of thermoregulation after exercise. *Journal of Applied Physiology*, 122: 933–944.

Kramer T, Garcia-Hansen V, Omrani S, et al. (2023). Personal differences in thermal comfort perception: Observations from a field study in Brisbane, Australia. *Building and Environment*, 245: 110873.

Li S, Zhang X, Li Y, et al. (2023). A comprehensive review of impact assessment of indoor thermal environment on work and cognitive performance - Combined physiological measurements and machine learning. *Journal of Building Engineering*, 71: 106417.

Lian Z (2024). Revisiting thermal comfort and thermal sensation. *Building Simulation*, 17: 185–188.

Lin Y, Jin H, Jin Y, et al. (2023). Experimental study on the effects of exercise intensity and thermal environment on thermal responses. *Building and Environment*, 232: 110067.

Liu G, Liang S, Hu S (2021). Calculation method of mean skin temperature weighted by temperature sensitivity of various parts of human body. *Journal of Thermal Biology*, 100: 102995.

Liu K, Dai Z, Zhang R, et al. (2022). Prediction of the sulfate resistance for recycled aggregate concrete based on ensemble learning algorithms. *Construction and Building Materials*, 317: 125917.

Marko D, Bahenský P, Bunc V, et al. (2022). Does Wim Hof method improve breathing economy during exercise? *Journal of Clinical Medicine*, 11: 2218.

Morozova N, Trias FX, Capdevila R, et al. (2022). A CFD-based surrogate model for predicting flow parameters in a ventilated room using sensor readings. *Energy and Buildings*, 266: 112146.

Motylinski M, MacDermott Á, Iqbal F, et al. (2022). A GPU-based machine learning approach for detection of botnet attacks. *Computers & Security*, 123: 102918.

Mou D, Cao B, Zhu Y (2022). Field study on thermal comfort of naturally ventilated residences in southwest China. *Journal of Central South University*, 29: 2377–2387.

Nishi Y (1981). Chapter 2 Measurement of thermal balance of man. In: Cena K, Clark JA (eds), Studies in Environmental Science, Vol. 10. Amsterdam: Elsevier. pp. 29–39.

Parsons K (2014). Human Thermal Environments: The Effects of Hot, Moderate, and Cold Environments on Human Health, Comfort, and Performance, Third Edition. Boca Raton, FL, USA: CRC Press.

Pedregosa F, Varoquaux G, Gramfort A, et al. (2011). Scikit-learn: Machine learning in Python. *The Journal of Machine Learning Research*, 12: 2825–2830.

Pekdogan T, Avci AB (2022). A field study on adaptive thermal comfort in a naturally ventilated design studio class in the post-pandemic period. *ALAM CIPTA International Journal of Sustainable Tropical Design and Practice*, 2: 80–86.

Périard JD, Eijsvogels TMH, Daanen HAM (2021). Exercise under heat stress: Thermoregulation, hydration, performance implications, and mitigation strategies. *Physiological Reviews*, 101: 1873–1979.

Qavidel Fard Z, Zomorodian ZS, Korsavi SS (2022). Application of machine learning in thermal comfort studies: A review of methods, performance and challenges. *Energy and Buildings*, 256: 111771.

Ramirez-Campillo R, García-Pinillos F, García-Ramos A, et al. (2018). Effects of different plyometric training frequencies on components of physical fitness in amateur female soccer players. *Frontiers in Physiology*, 9: 934.

Rao H, Shi X, Rodrigue AK, et al. (2019). Feature selection based on artificial bee colony and gradient boosting decision tree. *Applied Soft Computing*, 74: 634–642.

Rysanek A, Nuttall R, McCarty J (2021). Forecasting the impact of climate change on thermal comfort using a weighted ensemble of supervised learning models. *Building and Environment*, 190: 107522.

Sevilmis A, Özdemir İ, García-Fernández J (2023). The history and evolution of fitness. *SPORT TK-Revista EuroAmericana De Ciencias Del Deporte*, 12: 4.

Shi Y, Lian Z, Hu S, Hu Y (2022). Effects of multiple indoor environmental factors on anaerobic exercise performance. *Journal of Thermal Biology*, 108: 103280.

Simmons GH, Wong BJ, Holowatz LA, et al. (2011). Changes in the control of skin blood flow with exercise training: Where do cutaneous vascular adaptations fit in? *Experimental Physiology*, 96: 822–828.

Singh SK, Rai N, Subramanian A (2023). Machine learning-informed predictive design and analysis of electrohydrodynamic printing systems. *Advanced Engineering Materials*, 25: 2300740.

Tartarini F, Schiavon S, Cheung T, et al. (2020). CBE Thermal Comfort Tool: Online tool for thermal comfort calculations and visualizations. *SoftwareX*, 12: 100563.

Vargas NT, Chapman CL, Johnson BD, et al. (2018). Skin wettedness is an important contributor to thermal behavior during exercise and recovery. *American Journal of Physiology Regulatory, Integrative and Comparative Physiology*, 315: R925–R933.

Vellei M, de Dear R, Inard C, et al. (2021). Dynamic thermal perception: A review and agenda for future experimental research. *Building and Environment*, 205: 108269.

Wang Z, Yu H, Luo M, et al. (2019). Predicting older people's thermal sensation in building environment through a machine learning approach: Modelling, interpretation, and application. *Building and Environment*, 161: 106231.

Wang W, Ding G, Wang Y, et al. (2022). Field study on the effect of space type, exercise intensity, and wet bulb globe temperature on thermal responses of exercisers. *Building and Environment*, 225: 109555.

Weavil JC, Thurston TS, Hureau TJ, et al. (2022). Impact of aging on the work of breathing during exercise in healthy men. *Journal of Applied Physiology*, 132: 689–698.

Yang R, Zhang H, You S, et al. (2020). Study on the thermal comfort index of solar radiation conditions in winter. *Building and Environment*, 167: 106456.

Yang B, Li X, Liu Y, et al. (2022a). Comparison of models for predicting winter individual thermal comfort based on machine learning algorithms. *Building and Environment*, 215: 108970.

Yang Y, Yuan Y, Han Z, Liu G (2022b). Interpretability analysis for thermal sensation machine learning models: An exploration based on the SHAP approach. *Indoor Air*, 32: e12984.

Zaniboni L, Pernigotto G, Toftum J, et al. (2020). Subjective and objective assessment of thermal comfort in physiotherapy centers. *Building and Environment*, 176: 106808.

Zhai Y, Elsworth C, Arens E, et al. (2015). Using air movement for comfort during moderate exercise. *Building and Environment*, 94: 344–352.

Zhai Y, Zhao S, Gao Y, et al. (2020). Preferred Temperatures with and without Air Movement during Moderate Exercise. *Energy and Buildings*, 207: 109565

Zhang F, de Dear R, Hancock P (2019). Effects of moderate thermal environments on cognitive performance: A multidisciplinary review. *Applied Energy*, 236: 760–777.

Zhang S, Cheng Y, Olaide Oladokun M, et al. (2020a). Improving predicted mean vote with inversely determined metabolic rate. *Sustainable Cities and Society*, 53: 101870.

Zhang Y, Liu J, Zheng Z, et al. (2020b). Analysis of thermal comfort during movement in a semi-open transition space. *Energy and Buildings*, 225: 110312.

Zhang Y, Zhou X, Zheng Z, et al. (2020c). Experimental investigation into the effects of different metabolic rates of body movement on thermal comfort. *Building and Environment*, 168: 106489.

Zhou X, Xu L, Zhang J, et al. (2020). Data-driven thermal comfort model via support vector machine algorithms: Insights from ASHRAE RP-884 database. *Energy and Buildings*, 211: 109795.

Zhou X, Lai D, Chen Q (2021). Evaluation of thermal sensation models for predicting thermal comfort in dynamic outdoor and indoor environments. *Energy and Buildings*, 238: 110847.

Zhou X, Xu L, Zhang J, et al. (2022). Development of data-driven thermal sensation prediction model using quality-controlled databases. *Building Simulation*, 15: 2111–2125.

Zhou H, Xie D, Xiao P (2023). Research on thermal comfort of obese and overweight people during indoor running exercise. *Building and Environment*, 242: 110574.

Zora S, Balci GA, Colakoglu M, et al. (2017). Associations between thermal and physiological responses of human body during exercise. *Sports*, 5: 97.